Int J Thermophys (2017) 38:121
DOI 10.1007/s10765-017-2251-5

CPPTA3

Elastic Evaluation of Poly(Lactic Acid) Electrospun Membranes Using the Pulsed Photoacoustic Technique

M. Navarrete[1] · R. Vera-Graziano[2] · A. Maciel-Cerda[2] · F. M. Sánchez-Arévalo[2] · F. A. Godínez[3]

Received: 31 October 2016 / Accepted: 16 May 2017 / Published online: 6 June 2017

Abstract Fibrous membranes manufactured by electrospinning possess unique features such as a high porosity and large specific surface area, making them suitable for applications in tissue engineering. However, the determination of their mechanical behavior under different loading conditions remains one of the most difficult technical problems for researchers to overcome. While the tensile properties of this kind of membrane are commonly reported in the literature, few explorations of their properties in other directions have been reported. In this paper, the pulsed photoacoustic technique is employed to obtain the elastic constants of electrospun non-woven membranes, specifically in two directions (L, T). The electrospun samples are hybrid fiber membranes of poly(lactic acid) and hydroxyapatite (HA) nanoparticles at different concentrations. It is found that the concentration of HA nanoparticles determines the mechanical response of the membrane, where the nanoparticles act either as a reinforcement or as a mesh defect. The elastic constants (E_L, E_T, G_L, G_T, υ_L, ν_T) are obtained through velocity waves related to the stress–strain equations, using samples with two different geometries and considering the electrospinning mats as a transversely isotropic material. These values are compared to those acquired using macro-tensile testing equipment according to the ASTM D1708 standard.

Selected papers from Third Conference on Photoacoustic and Photothermal Theory and Applications.

✉ M. Navarrete
mnm@pumas.iingen.unam.mx

1 Instituto de Ingeniería, Edificio 12 Circuito Exterior, C. U., Universidad Nacional Autónoma de México, Av. Universidad 3000, 04510 Mexico City, Mexico

2 Instituto de Investigación en Materiales, Universidad Nacional Autónoma de México, 04510 Mexico City, Mexico

3 Instituto Tecnológico de Chihuahua, C. P. 31310 Chihuahua, Mexico

Graphical Abstract

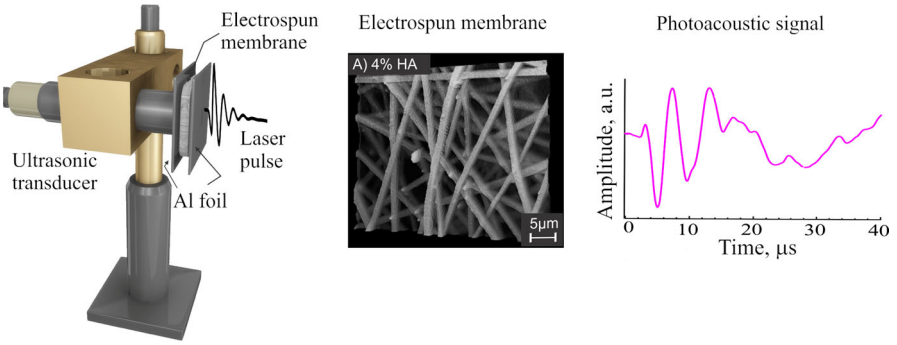

Keywords Electrospinning · Electrospun composites · Fiber membranes · Mechanical properties · PLA–hydroxyapatite · Pulsed photoacoustic technique

1 Introduction

Tissue bioengineering, which has been an active research area for several decades, requires materials with tailored properties for physical, chemical, biological, mechanical functionalities and sometimes must include a tuning mechanism for both the short- and long-term degradation rates. All of these characteristics must be satisfied for the specific application, e.g., prosthetic devices, implants, vascular grafts, catheters, sutures, and ligament repair [1,2]. As a tissue turns over, the implanted scaffold must conserve its stability and promote cell growth and proliferation, keeping up with the gradual degradation along with the construction of new tissue, where the scaffold is eventually completely replaced. Examples of biodegradable materials are aliphatic polyesters such as poly(ε-caprolactone), poly(lactide)s, poly(glycolide) and their copolymers, which are being extensively investigated for medical and pharmaceutical applications [3]. These synthetic and natural polymers fulfill the design requirements when arranged into fiber networks. Among the methods for the manufacturing of fibers on the nano-/micrometer scale (in terms of diameter), electrospinning is perhaps the most versatile process for the production of electrospun membranes. The resemblance of the physical structure to a biological extra cellular matrix (ECM) is a unique advantage of an electrospun scaffold; due to the nanometric scale, the ECM fibrils and their porous structure may be mimicked using a special electrospinning process [4,5].

The use of electrospinning began in 1934, when Formhals published five patents describing an experimental setup for the production of polymer filaments using an electrostatic force. An electric field applied between a needle and a collector generates a charged jet of polymer solution, and as the jet travels air, the solvent evaporates, leaving behind a charged fiber that is collected on a metal screen forming an electrospun web in a flat plane (sheet of tangled single thread); this plane can be considered a single phase, and its successive staking produces nano- or microfiber non-woven membranes [6].

Table 1 Mechanical properties for PLA and PLA/HA electrospun membranes, including their tensile strength and ultimate strain found in the literature

Material	Tensile strength (MPa)	Elastic modulus (MPa)	References
PLA	4.69 ± 0.19	–	[7]
PLA/HA	3.10 ± 0.15	–	[7]
PLA	1.40 ± 0.11	12 ± 2	[8]
PLA/HA	2.86 ± 0.24	118 ± 10	[8]
PLA bulk	53–70	5000–4800	[1,9]
PLA film	31 ± 01	1030 ± 50	[10]
PLA single fiber	–	2000–8000	[11]

Poly(lactic acid) or polylactic acid or polylactide (PLA) is a biodegradable and bioactive thermoplastic that involves the processing and polymerization of lactic acid monomer. Lactic acid is a chiral molecule which exists as two enantiomers, L- and D-lactic acid, differing in their effect on polarized light

When the diameter of the polymer fiber is reduced from micrometers to nanometers, its morphology is modified, and it shows a superior mechanical behavior (e.g., stiffness and tensile strength) compared to the bulk material [3,4].

The 2D fibrous membranes display a high density of surface defects (introduced during electrospinning), and aspects such as porosity, morphology, fiber arrangement, and others characteristics cause the fibrous polymeric membranes to exhibit different effective mechanical properties as shown in Table 1 for the PLA/HA electrospun composites.

These differences are mainly due to the fact that these materials cannot be classified as either bulk materials or thin films, but rather are heterogeneous materials because of their high porosity and non-uniform density and thickness. Thus, to assess their mechanical properties experimentally, it is necessary to use modifications that change their configuration, conformation, and sometimes even their boundary conditions. For example, when a membrane is prepared for tensile strength testing, it must be die- cut to the standard geometry according to the appropriate ASTM standard, or when the three-point bending technique using a single fiber is used, the fiber–fiber interaction is suppressed (surface forces, connectivity, jamming, etc., [12]). Load transfer is another challenge in such systems; effective load transfer will never be realized because these materials do not have a support matrix as in true composite materials. Therefore, it is necessary to use other methods to achieve stability and provide effective load transfer so that these kind of materials can be effectively characterized; one example is the photoacoustic technique, in which a laser pulse is used as a standard source of ultrasound, and the velocity of the resulting waves is related to the stress–strain equations.

In the present study, the macro-traction and pulsed photoacoustic measurement techniques are applied to obtain the elastic constants in two directions of the fiber membranes of poly(L-lactic acid) (PLA) with inclusions of hydroxyapatite (HA) nanoparticles at different concentrations that were produced by electrospinning. Both of the experimental techniques used to obtain the values of the elastic constants are

compared and discussed with respect to the physical characteristics of electrospun membranes.

1.1 Theoretical Considerations

To determine the elastic constants of the electrospun membranes, we use the photoacoustic technique in which a laser pulse is applied on a metal thin film to produce a localized excitation and generate acoustic waves that propagate into the sample. The velocity of these waves is related to the stress–strain equations of the elastic solids. For the analysis of the electrospun membranes, it is assumed that the material possesses transverse isotropic behavior [13–17]; under this assumption, the number of elastic constants is reduced to six, of which five are independent constants. These five constants are: E_{L} (Young's modulus in the plane of the transverse isotropy), E_{T} (Young's modulus in a direction normal to the plane of the transverse isotropy), G_{T}(shear modulus in the planes normal to the plane of the transverse isotropy), and ν_{L}, ν_{T} (Poisson's ratios characterizing the lateral strain response in the plane of the transverse isotropy to a stress acting parallel and normal to it, respectively), as shown in Fig. 1.

1.2 Density Determination

The determination of the elastic constants from the acoustic velocities requires a priori knowledge of the density in each direction; this property is assumed to be constant for homogeneous, isotropic materials. However, as observed in microstructural characterization, our samples are heterogeneous and anisotropic. As a result, the accurate determination of the density of these electrospun membranes is a difficult task. As a first approximation, we measured the weight and thickness of the samples with known geometry; however, these values must be corrected taking into account the theory of porous media [18–20].

1.3 Calculation of the Elastic Constants of Electrospun Membranes

The longitudinal elastic moduli in the L and T directions, E_L and E_T, are calculated from the acoustic wave velocities using the k ratio [21]. Here, k is defined as: $k = C_1/C_2$ where C_1 is the longitudinal wave velocity in the L or T direction, and C_2 is the shear wave velocity measured in the L or T direction or by considering the arrival times of the longitudinal and transverse waves.

The values of the elastic moduli in the L and T directions are determined using the classical acoustic equation $E_L = E_T = \frac{\rho C_2^2(4-3k^2)}{1-k^2}$. Due to the unstable fibrous morphology of the electrospun membranes, the samples are prepared with a cylindrical geometry to obtain the elastic modulus values in the direction L. Additionally, we consider the quasi-longitudinal compressional waves for which the transverse stresses are zero, but the transverse strains are not; these waves propagate at a speed given by $C_L = (M/\rho)^{1/2}$ where M is known as the acoustic modulus, and ρ is the material density [14].

2 Materials and Procedures

2.1 Samples and Characteristics

2.1.1 Material

Chemicals: L-lactide (PURAC biomaterials) was purified by crystallization with ethyl acetate in vacuum. Poly(L-acid lactic) (PLLA, *Mw* 280 000/NatureWorks LLC). Hydroxyapatite nanoparticles, HA, (particle size <200 nm)/Sigma-Aldrich). 2,2,2-trifluoroethanol, TFE, O-xylene anhydride and chloroform (Sigma-Aldrich). The solvents were used as received.

2.1.2 Solvent Casting and Electrospinning Procedure

Blend solutions were obtained by dissolving PLA and HA granules in TFE at different weight ratio, i.e., 90/10, 80/20, and 70/30 % (v/w), with the overall concentration fixed at 16 % (w/v). All solutions were stirred magnetically at 25 °C and 20 rpm. The solutions were poured into a glass syringe and electrospun in the steady flow rate regime using a high-voltage power supply (Spellman, USA) and a digitally controlled syringe pump (KD Scientific, USA) in the following conditions: flow rate of 0.6 ml/h and applied voltage of 5 kV. The process was carried out in air at room temperature. Polymeric mats were collected on a fixed grounded aluminum target (10 cm square) located 30 cm from the bunt tip of the capillary. Finally, electrospun membranes were dried by vacuum for 48 h at 40 °C and were then stored in a desiccator.

2.1.3 Microstructural Characteristics of Electrospun Membranes

The electrospun membranes exhibit an external surface resembling a random non-woven mat, as well as a quasi-layered structure as shown in Fig. 1. Its high inherent porosity and its layered configuration imply the presence of interfaces at different scales that have an inhomogeneous effect on its mechanical behavior. When the handling of these membranes is conducted with a substrate, an aluminum foil is used. Microstructural analysis was performed using scanning electron microscopy (SEM) (Leica Cambridge Stereoscan 440). The average fiber diameter and voids size esti-

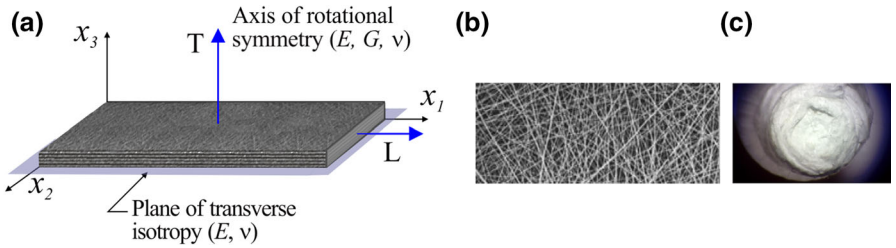

Fig. 1 Morphological aspects of the PLA electrospun membranes. Schematic diagrams: (a) laminate mat coordinate system; (b) layer structure; and (c) photograph of a mat sample rolled in a cylindrical shape

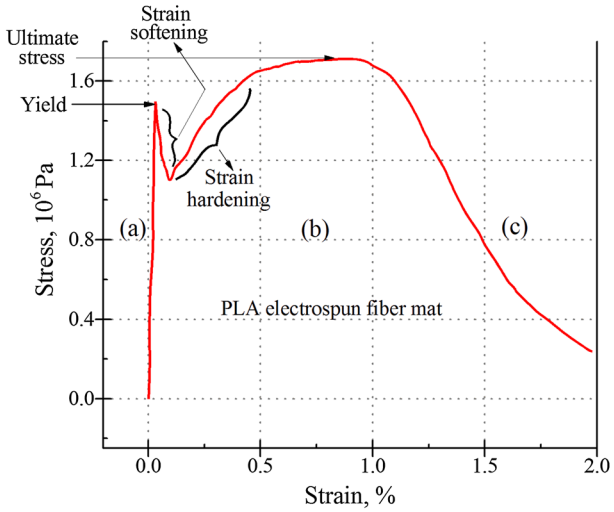

Fig. 2 Stress–strain response of a PLA electrospun fiber mat sample deformed under uniaxial tension. The accompanying images show the PLA structure at various % of strain; regions: (a) linear-elastic; (b) no linear behavior; and (c) rupture

mation were calculated randomly by selecting approximately 35 fibers in the SEM micrographs using the ImageJ software package.

2.2 Tensile Testing

Uniaxial tensile tests were carried out on dog-bone specimens cut out from each electrospun mat using a stainless steel die (gauge length: 26 mm; width: 6 mm; tolerance: ± 0.05 mm) according to ASTM D 1708 [22]. Mechanical tests were performed at 10 mm/min to rupture using a 110 N load cell. Five samples were analyzed for each HA concentration. The samples showed a variation in their thickness ranging between 0.04 mm and 0.1 mm. Y_L (Tensile modulus), yield strength, and ultimate tensile stress of the samples were determined from the stress–strain curves. Figure 2 shows a stress–strain curve obtained for a sample of a PLA electrospun fiber mat with inserted images of the mechanical behavior under tension. As shown in the figure, this material undergoes significant nonlinear elongation prior to rupture, which means that it behaves as a ductile material.

2.3 Wave Propagation Testing

Due to the physical characteristics of the membranes, it is necessary to use a most powerful mechanism to generate ultrasound "ablation regimen," such that only small quantities of material are ejected from the surface. In this way, the samples are prepared so that the energy of the laser pulse, under ablative conditions, does not strike them directly. Thus, the ablative laser pulse is absorbed either by an aluminum foil or an

aluminum rod where the waves are generated and transferred to the sample without coupling (e.g., by grease), but under constrained conditions due to mechanical pressure transmitted by the sample holder.

2.3.1 Equipment Used for Laser-Induced Ultrasound

A Nd:YAG pulsed laser with a Gaussian spatial and temporal distribution at 10 Hz, $\lambda = 1064$ nm, pulse energy of 200 mJ and length of 6 ns with the spot diameter of 4.5 mm is used for ultrasonic wave generation. A piezoelectric PZT transducer (General Electric) is used as receiver for the photoacoustic (PA) signals, and its characteristics are: bandwidth from 6.7 MHz to 12.45 MHz (at the –6 dB), peak frequency 9 MHz, and central frequency 9.56 MHz, with output still visible past 15 MHz. The PA signals are acquired and stored using a digital oscilloscope (1 GHz, Lecroy) that is triggered by the laser pulse. In Fig. 5, the waveform indicated as (ii) shows the piezoelectric transducer response to the laser pulse; this waveform has small oscillations in its tail, which means that the transducer has internal resonance due to its high frequency, backing layer material, and impedance mismatches. This internal resonance will add a ringing effect to the acquisition as seen in profile (iii) which is the response when the sample holder is added; however, this noise almost disappears when the sample is added because the impedance mismatches decrease, as shown in profile (iv).

2.3.2 Preparation of the Samples

Our electrospun membranes simultaneously exhibit a fibrous and the laminate structure. Therefore, we expected a further delay in the propagation of waves through the membrane in the T direction relative to that in the L direction. This is due to the fact that in the former case, the interfaces act as scattering zones, whereas in the latter case, they act as waveguides.

Taking into account the effects described above, we consider the electrospinning membrane as a *transversely isotropic material* with the plane of isotropy defined by $x_1 - x_2$ (see Fig. 1a). Accordingly, the samples are prepared in two different geometries with five samples for each HA concentration.

a) *To determine the values for the elastic constants in the T direction*. The membrane is held between two layers of aluminum foil ($102.09 \pm 4.44\mu$m in thickness) with a glass slide ($25 \times 75 \times 1.1$ mm, 90° ground edges, plain) on each side, used for support, as shown in Fig. 3. The average values obtained for the physical properties are displayed in Table 2.

b) *To determine the values for the elastic constants in the L direction*. The mat is wound into a cylindrical shape, wrapped in Mylar foil, and then placed inside the glass tube (inner diameter of 6 mm) to fix. A short metal rod (with the same diameter as that of the rolled membrane) on each side of the cylindrical sample is attached to ensure the propagation of the acoustic waves, as shown in Fig. 4. For this configuration, the samples behave as a short bar, and the average measured values of the physical properties are displayed in Table 3.

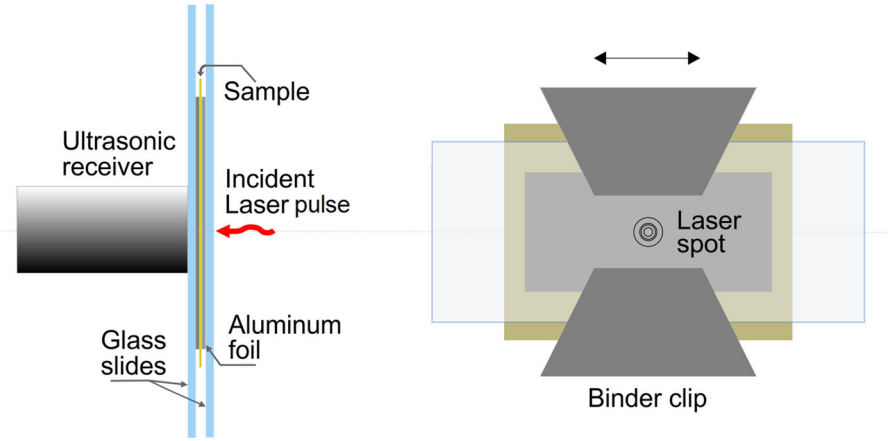

Fig. 3 Mechanical arrangement for fixing the sample to acquire the photoacoustic signals in the T direction

Table 2 Average physical properties of the flat samples cut out from each electrospun mat

Flat sample	[a]Average fiber diameter (μm)	[b]Porosity (%)	Thickness (μm)	Weight (mg)	Density (kg/m^3)
PLA/HA_00	0.77 ± 0.06	44.2	359 ± 14	65 ± 3	190 ± 06
PLA/HA_04	0.73 ± 0.12	40.4	253 ± 20	46 ± 4	196 ± 10
PLA/HA_10	0.88 ± 0.12	40.8	349 ± 12	60 ± 3	183 ± 13
PLA/HA_20	0.84 ± 0.15	49.6	358 ± 08	70 ± 1	209 ± 07
PLA/HA_30	0.92 ± 0.16	56.3	302 ± 13	57 ± 1	208 ± 36

[a] Mean diameter of individual fibers as well as average porosity of the membrane obtained via digital image processing from SEM micrographs.
[b] Porosity volume fraction calculated by the Image J software package

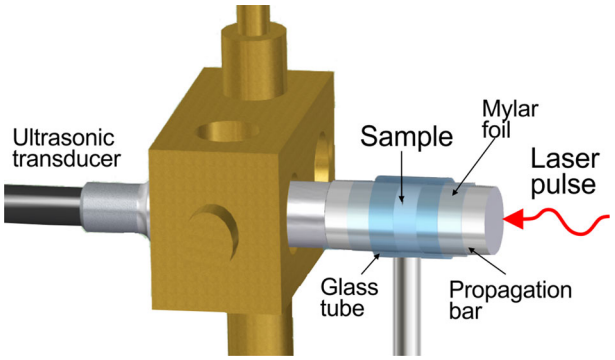

Fig. 4 Mechanical arrangement for fixing the sample to acquire the photoacoustic signals in the L direction

Table 3 Average physical properties of the rolled-up samples cut out from each electrospun mat

Cylindrical sample	Weight (mg)	Thickness (mm)	Density (Kg/m^3)
PLA/HA_00	30.5 ± 0.1	3.74 ± 0.12	293 ± 14
PLA/HA_04	24.8 ± 4.0	3.40 ± 0.01	262 ± 42
PLA/HA_10	22.2 ± 2.6	2.88 ± 0.32	264 ± 21
PLA/HA_20	24.4 ± 2.0	2.55 ± 0.20	344 ± 40
PLA/HA_30	25.4 ± 1.2	1.80 ± 0.70	560 ± 50

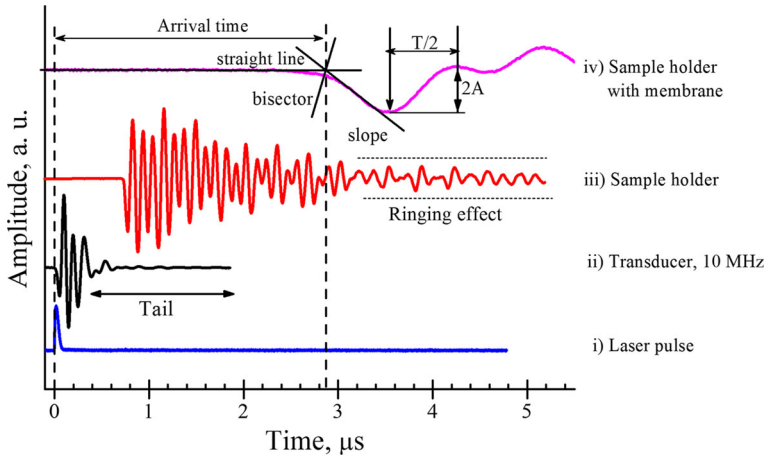

Fig. 5 Arrival times of the PA signals in the T direction for each interface that is added in the signal's trajectory. The corresponding geometric arrangement is shown in Fig. 3. (*i*) Laser pulse waveform; (*ii*) piezoelectric transducer output signal generated by the excitation of the laser pulse; (*iii*) PA signal generated by the sample holder, without sample, showing the ringing effect; and (*iv*) PA signal output with the sample fixed inside of the sample holder

2.3.3 Adjustments to the PA Signals

In our case, the retardation of the acoustic wave is due not only to the physical characteristics of the membrane but also to the properties of the sample holder, which should be considered for the determination of the elastic constants of the samples.

Thus, the average correction time for the T direction is approximately 0.8 μs, while that for the L direction is approximately 6 μs. Figure 5 shows the shift of the PA signal output for each interface that is added in the signal's trajectory, given the geometric arrangement shown in Fig. 3.

3 Results and Discussion

Our electrospun membranes exhibit a laminate structure; each layer is forming from a long fiber drawn without preferential direction and constituting a tangled layer with a non-uniform thickness. Repetition of this production process gives rise to the stacking

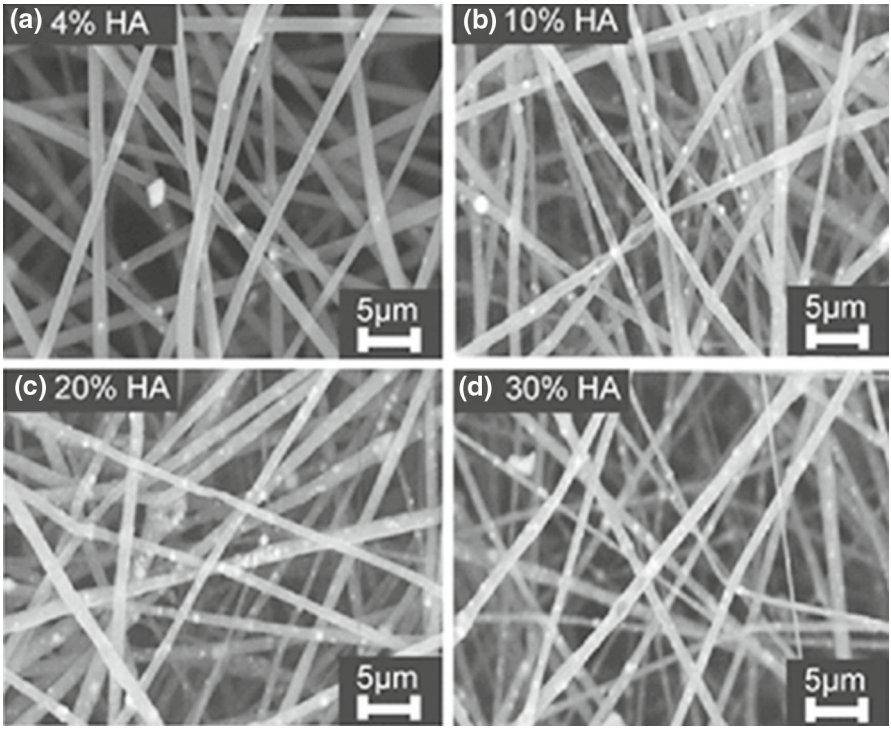

Fig. 6 Micro-morphological aspects of the PLA/HA electrospun membranes. SEM micrographs showing different concentrations of HA nanoparticles: (a) 4 %; (b) 10 %; (c) 20 %; and (d) 30 % w/w. The HA nanoparticles are imaged as light spots

and overlapping of these layers forming an important material known as a microporous membrane. Figure 6 presents the SEM micrographs of four electrospun membrane samples loaded with 4, 10, 20, and 30 % w/w of HA nanoparticles. The bright spots on the fibers correspond to the HA locations. From these micrographs, it can be observed that: a) the fibers accumulate in specific zones, and b) the HA nanoparticles show different distribution along the fibers. Both characteristics are a qualitative indication of a complex anisotropy. The fiber diameters range from 0.87 to 1.45 microns. The diameter of the fibers decreases slightly as the HA content increases. This decrease in mean diameter is most likely due to the viscosity change in the blend solutions. Furthermore, this kind of electrospun membrane exhibits hydrophilic and electrostatic properties, and its boundaries adsorb and retain water and impurities from the surrounding air; therefore, it is necessary to stabilize these membranes with other materials.

The average numerical values of the elastic properties of the electrospun membranes, in both the L and T directions, as a function of HA volume fraction, and other pertinent results are presented in Tables 4 and 5.

Examination of the E_L and E_T values as a function of HA concentration shows that an increase in the HA loading significantly decreased the E_T values, while the tensile properties Y_L remained almost unaltered.

Table 4 Mechanical properties in the L direction

Procedure	[a]Pulsed photoacoustic						[b]Macro-tensile measurements	
Cylindrical sample	Longitudinal velocity (m/s)	k	M_L (MPa)	E_L (MPa)	G_L (MPa)	ν_L	Y_L (MPa)	Ultimate tensile (MPa)
PLA/HA_00	710 ± 212	2.3 ± 0.14	142	33 ± 02	12 ± 01	0.36 ± 0.05	98 ± 33	3 ± 0.6
PLA/HA_04	630 ± 138	1.9 ± 0.14	137	42 ± 10	16 ± 04	0.31 ± 0.02	90 ± 32	2 ± 0.5
PLA/HA_10	710 ± 108	2.6 ± 0.41	167	19 ± 05	6.8 ± 04	0.30 ± 0.10	98 ± 31	1 ± 0.5
PLA/HA_20	606 ± 116	2.6 ± 0.80	121	17 ± 05	6.2 ± 04	0.37 ± 0.11	98 ± 44	1.8 ± 0.3
PLA/HA_30	1020 ± 173	2.5 ± 0.5	189	24 ± 08	09 ± 044	0.33 ± 0.05	89 ± 304	1.4 ± 0.4

[a] Average value of the elastic constants calculated using the pulsed photoacoustic technique data.
[b] Macro-tensile measurement on PLA electrospun membranes. Y_L, ultimate tensile: average value for the longitudinal Young's modulus of the membranes obtained via MTS universal testing machine

Table 5 Mechanical properties in the T direction using pulsed photoacoustic technique data

Flat samples	Longitudinal velocity (m/s)	k	M_T (MPa)	E_T (MPa)	G_T (MPa)	v_T
PLA/HA_00	134	1.3 ± 0.1	3.4	4.25 ± 1.65	2.12 ± 0.22	0.002
PLA/HA_04	132	1.2 ± 0.1	3.4	2.48 ± 0.60	2.49 ± 0.40	–
PLA/HA_10	134	1.5 ± 0.3	3.4	1.45 ± 0.31	0.90 ± 0.10	–
PLA/HA_20	120	1.7 ± 0.1	3.1	1.76 ± 0.90	0.90 ± 0.22	0.02
PLA/HA_30	151	1.5 ± 0.1	4.5	3.34 ± 0.08	1.51 ± 0.11	0.01

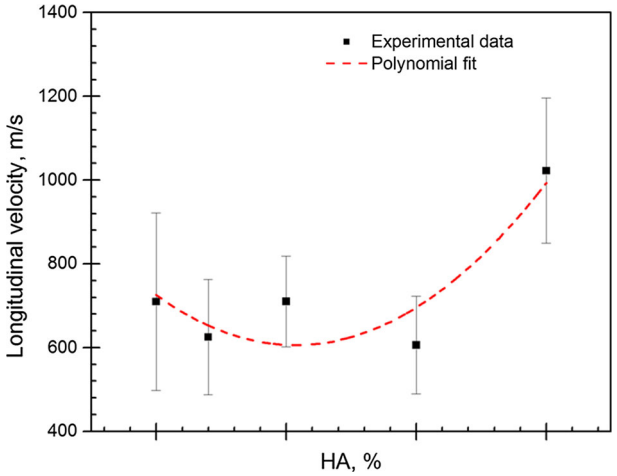

Fig. 7 Profile of the longitudinal velocity in the L direction as a function of the volume fraction of HA. Each experimental point is an average obtained from five samples with the same physical characteristics and concentration of HA

The tensile strength and ultimate strength decrease with increasing HA; additionally, the data presented in Fig. 6 show that HA nanoparticles are deposited in a non-uniform distribution along the microfibers forming amalgamations that in turn can be a source of stress concentration.

Figure 7 shows the behavior profile for the longitudinal velocity in the L direction, in which low concentrations of HA nanoparticles behave as defects and at higher values behave as reinforcements.

However, the elastic constants reported in this paper are slightly lower than those reported in the literature; this is generally due to the variation in conditions during the production process. The average values are on the same order of magnitude, as shown in Table 1.

4 Conclusions

The determination of the elastic constants in two directions using different geometric arrangements has been demonstrated by considering that the electrospun membranes behave as transversely isotropic materials.

The properties and performance of electrospun membranes with nanoparticles depend on the geometric attributes of the fibers such as the volume fraction, density, and size distribution, as well as on the spatial arrangement of the long fiber in the air matrix. When another phase such as the HA nanoparticles is included in the blend solution, these particles are not uniformly distributed within the long fiber, changing its mechanical behavior. We found that depending on the concentration of the particles, they behave as defects or reinforcements.

Moreover, the mechanical properties in the T direction are the specific data that will allow the design of membranes with sufficient mechanical strength to withstand the weight of the cells.

Acknowledgements This work was supported by DGAPA-PAPIIT-UNAM under Grants IN106515, IN105117 and IN108116 as well by II-UNAM under Grant 6593.

References

1. L.S. Nair, C.T. Laurencin, Prog. Polym. Sci. **32**, 762 (2007)
2. M. Yao, H. Deng, F. Mai, K. Wang, Q. Zhang, F. Chen, Q. Fu, Express Polym. Lett. **5**, 937 (2011)
3. B. Gupta, N. Revagade, J. Hilborn, Prog. Polym. Sci. **32**, 455 (2007)
4. V. Beachley, X. Wen, Prog. Polym. Sci. **35**, 868 (2010)
5. H. Zheng-Ming, Y.-Z. Zhang, M. Kotaki, S. Ramakrishna, Compos. Sci. Technol. **63**, 2223 (2003)
6. J. Zeleny, Phys. Rev. **10**, 1 (1917)
7. C. Wang, H.S. Chien, K.W. Yan, C.L. Hung, K.L. Hung, S.J. Tsai, Polymer **50**, 6100 (2009)
8. P.P. Molamma, J. Venugopal, S. Ramakrishna, Acta Biomater. **5**, 2884 (2009)
9. G. Sui, X. Yang, F. Mei, X. Hu, G. Chen, X. Deng, S. Ryu, J. Biomed. Mater. Res. A **82**, 445 (2006)
10. J.H. Chang, Y.U. An, D. Cho, E.P. Ginnelis, Polymer **44**, 3715 (2003)
11. C.L. Pai, M.C. Boyse, G.C. Rutledge, Polymer **52**, 2295 (2011)
12. F. Croisier, A.-S. Duwez, C. Jérome, A.F. Leonard, K.O. van der Werf, P.J. Dijkstra, M.L. Bennink, Acta Biomater. **8**, 218 (2012)
13. J.J. Liao, T.-B. Hu, C.-W. Chang, Int. J. Rock Mech. Min. Sci. **34**, 1045 (1997)
14. T.D. Rossing, D.A. Russell, Am. J. Phys. **58**, 1153 (1990)
15. M. Navarrete, M. Villagrán, Rev. Sci. Instrum. **74**, 479 (2003)
16. M. Navarrete, R. Vera-Graziano, J. Pineda, J. Appl. Polym. Sci. **111**, 1199 (2009)
17. M. Navarrete, F. Serranía, M. Villagrán, J. Bravo, R. Guinovart, R. Rodríguez, Mech. Adv. Mater. Struct. **9**, 157 (2002)
18. E.H. Kerner, Proc. Phys. Soc. B **69**, 808 (1956)
19. W.M. Madigosky, R.W. Harrison, K.P. Scharnhorst, Polym. Mater. Sci. Eng. **60**, 489 (1989)
20. R.L. Kligman, W.M. Madigosky, J.R. Barlow, J. Acoust. Soc. Am. **70**, 1437 (1981)
21. C.B. Scruby, L.E. Drain, in *Laser Ultrasonics: Techniques and Applications*, ed. by C.B. Scruby, L.E Drain (Hilger, Neew York, 1990)
22. ASTM D1708-10, Standard test method for tensile properties of plastics by use of microtensile specimen. ASTM 08.01 Plastics (I): D256–D3159 (2011)